Electronic Supplementary Material (ESI) for Nanoscale Horizons.

Supporting Information

Boosting efficiency of luminescent solar concentrators using ultra-bright carbon dots with large Stokes shift

Jiurong Li[a], Haiguang Zhao*[,b], Xiujian Zhao[a], and Xiao Gong*[,a]

a. State Key Laboratory of Silicate Materials for Architectures, Wuhan University of Technology, Wuhan 430070, P. R. China.
b. State Key Laboratory of Bio-Fibers and Eco-Textiles & College of Textiles & Clothing, Qingdao University, No. 308 Ningxia Road, Qingdao 266071, P. R. China.

* Corresponding authors:

E-mail address: hgzhao@qdu.edu.cn (H. Zhao); xgong@whut.edu.cn (X. Gong)

1. Experimental section

Materials

Resorcinol (Rc), m-phenyldimethylamine (mPDA), and polyvinylpyrrolidone (PVP), were supplied by Aladdin Chemistry Co., Ltd., China. Absolute ethanol was supplied by Sinopharm Chemistry Reagent Co., Ltd., China.

Synthesis of yellow emissive CDs

Yellow emissive CDs were prepared via a solvothermal method as following: 1.0 mmol of Rc was dissolved in 10 mL of absolute ethanol, the mixture was sonicated for 15 minutes. After the mixture was completely dissolved, 1 mL of mPDA was added, and the mixture was subsequently transferred to a poly(tetrafluoroethylene) (Teflon)-lined autoclave (25 mL) and heated at 180 ^{o}C for 6 h. The reactor was automatically cooled to room temperature and the solution was gently removed. Subsequently, the as-fabricated yellow emitting CDs were first purified by filtration using polycarbonate membrane filters (from Filter-Lab) with a pore size of 0.22 μm, and the supernatant was collected to achieve removal of the unreacted reagents. Finally, the sample was used to further characterization and LSC device applications.

Synthesis of non N-doped CDs

The whole synthesis process was the same as that of yellow emitting CDs, except that no nitrogen doping source was added.

Fabrication of thin-film CD-polymer LSCs

Different concentrations of CDs (20 mg/mL, 40 mg/mL, 60 mg/mL, 80 mg/mL and 100 mg/mL) were dispersed in PVP ethanol solutions (PVP K30 concentration:

90 mg/mL and PVP K90 concentration of 90 mg/mL). First, the mixture of ethanol and PVP was stirred for 24 h in order to obtain a clear solution. After adding the different concentrations of CDs, the mixture was blended continuously to the appropriate blending time. Subsequently, the mixture was centrifuged for 10 min at 6000 r.p.m. to obtain a bubble-free solution. The solution was further drop-casted on the glass ($5 \times 5 \times 0.2$ cm^3 and $10 \times 10 \times 0.94$ cm^3) and dried at room condition for 1 h until all solvents was evaporated. In the end, a Si solar cell was mounted on edges of the LSC using epoxy glue.

Characterizations

Absorption spectra of CDs were recorded with a UV-Vis spectrophotometer (UV2600, Shimadzu Corp., Tokyo, Japan). PL spectra of CDs were measured at room temperature with a time-resolved fluorescence spectrometer (FL3-22, Jobin-Yvon, USA). The fluorescence delay was achieved by an automatic delay stage (M-ILS300LM, Newport, USA). Intensity of the pump light was directly measured using a power meter (Model 843-R, Newport). The focal size of pump beam (~0.1 mm) was measured using the beam profiler (LBP2-HR-VIS2, Newport, USA). The morphology of samples was measured by Transmission electron microscopy (TEM) using a JEM-2100F TEM (JEOL, Japan). Fourier transform infrared (FT-IR) spectra were recorded using a FT-IR spectrometer (Nicolet 6700, Thermo Electron Co., USA). The X-ray photoelectron spectroscopy (XPS) spectra of the samples were collected by using a Thermo Fisher Scientific ESCALAB 250Xi spectrometer equipped (USA). The X-ray diffraction (XRD) was performed using a D8 Advance diffractometer (Bruker,

Germany, Kα=1.5406 Å). A solution phase nuclear magnetic resonance (NMR) (Bruker, AVANCE III HD, 600 MHz) was used to characterize the ^{1}H NMR and ^{13}C NMR in DMSO-d_6. The mass spectra (MS) were analyzed using Bruker's MALDI-TOF-TOF (Ultraflextreme) device. Photovoltaic properties of LSCs were obtained with a solar simulator (IV4112, Newport Corp., Irvine, CA, USA) at an intensity of 100 mW·cm^{-2} (1 sun), calibrated through a calibrated silicon solar cell.

Theoretical simulation[1]

The η_{opt} of the LSCs is expressed as following based on the reported method:

$$\eta_{\text{opt}} = \eta_{Abs} \cdot \eta_{i\text{internal}} \tag{1}$$

Where η_{Abs} is the fraction of absorbed sunlight by the LSC and η_{internal} is the internal quantum efficiency of the LSC.

η_{Abs} can be calculated as:[1]

$$\eta_{\text{Abs}} = \frac{\int_0^{\infty} I_{in}(\lambda)\left(1 - e^{-\alpha(\lambda)d}\right)d\lambda}{\int_0^{\infty} I_{in}(\lambda)d\lambda} \tag{2}$$

In which α is the absorption coefficient calculated as $\alpha = \text{In}(10)\frac{A}{d}$, where d is the effective length, A the absorption of the LSC measured by the absorption spectra, and I_{in} is the Sun irradiance.

A spectrally averaged internal efficiency (η_{internal}) over the PL emission of the CDs was calculated as:

$$\eta_{\text{internal}} = \frac{\int_0^{\infty} \frac{\eta_{\text{QY}} P_{\text{TIR}}}{1 + \beta\alpha(\lambda) L_{\text{LSC}}\left(1 - \eta_{\text{QY}} P_{\text{TIR}}\right)} S_{\text{PL}}(\lambda)d\lambda}{\int_0^{\infty} S_{\text{PL}}(\lambda)d\lambda} \tag{3}$$

In which $S_{PL}(\lambda)$ is the PL emission spectrum; β is a numerical value fixed to 1.4 and L_{LSC} is the length of the LSC. Assuming an isotropic emission, P_{TIR} is defined by the escape cone identified by the critical angle θ of the air/glass interface:

$$P_{TIR} = \sqrt{1 - \left(\frac{n_{air}}{n}\right)^2} \qquad (4)$$

Calculation of the optical efficiency (η_{opt}): [1-4]

η_{opt} is defined as the number of photons emitted from the edges of the LSC divided by the number of photons incident on its top surface, it can be used to evaluate the energy generation feature of LSCs. In addition, η_{opt} is the key metric to evaluate the performance of LSCs. In generally, by attaching a photovoltaic cell at the end of the LSCs in order to estimate η_{opt} and measuring its short circuit current as given in equation (5).

In our case, we attached polycrystalline silicon solar cell on one edge of the LSC device.

$$\eta_{opt} = \frac{I_{LSC} \times A_{edge}}{I_{Si\,cell} \times A_{top}} \qquad (5)$$

Where I_{LSC} is the short-circuit current measured from the solar cell attached with the LSC device and $I_{Si\,cell}$ is the short circuit current measured from the same solar cell under direct illumination of the same light source. While A_{top} and A_{edge} are its top surface area and the area of its lateral face where the solar cell is attached. Ratio A_{top}/A_{edge} is generally termed as geometric gain (G). In case of our LSCs, the G is 6.25 for the size of 5 × 5 cm^2 and 2.5 for size of 10 × 10 cm^2. Additionally, we also calculated the overall power efficiency ($\eta_{overall}$) of LSC device using the formula given in equation (6).

$$\eta_{overall} = J_{sc} \times V_{oc} \times FF \qquad (6)$$

$$FF = \frac{V_{MP} \times I_{MP}}{V_{OC} \times I_{SC}} \qquad (7)$$

Where J_{sc} is the short circuit current density, V_{oc} is the open circuit voltage, *FF* is the fill factor calculated using equation (7) in which V_{MP} and I_{MP} are the voltage and current at the maximum power and I_{sc} is the short circuit current. To obtain the results, a LSC device was illuminated perpendicularly to its surface by the AM 1.5G solar simulator (100 mW cm^{-2}). Firstly, the solar cell was covered with black commercial tape, which contained a window, so that one face of the cuvette could be placed in contact with the solar cell, while the remaining part of solar cell was blocked from receiving light. Secondly, because of the presence of LSC with additional electrical wiring, the transparent tape was also used to maintain the mechanical stability of device.

PCEs of the LSCs

The custom-sized Si photovoltaic was attached on one edge of the LSC by glass glue, and the rest of the edges were uncovered. The uncovered part of the photovoltaic was blocked by the black tapes to avoid any incident light. Then the LSC was placed under a conventional AM 1.5G solar simulator with illumination perpendicular to the surface of the LSC. No reflector or back diffuser was put beneath the device.

2. Results:

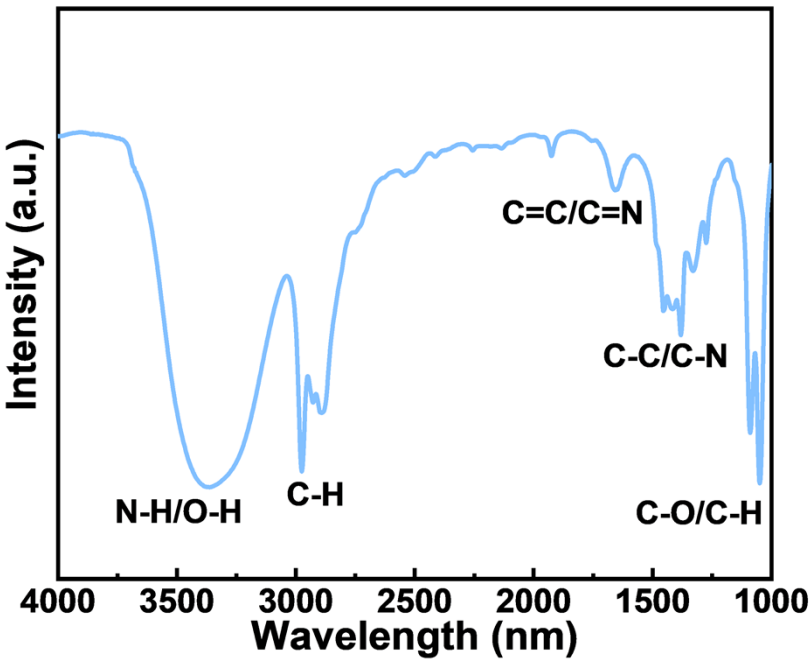

Figure S1. FTIR spectra of the synthesized yellow emitting CDs.

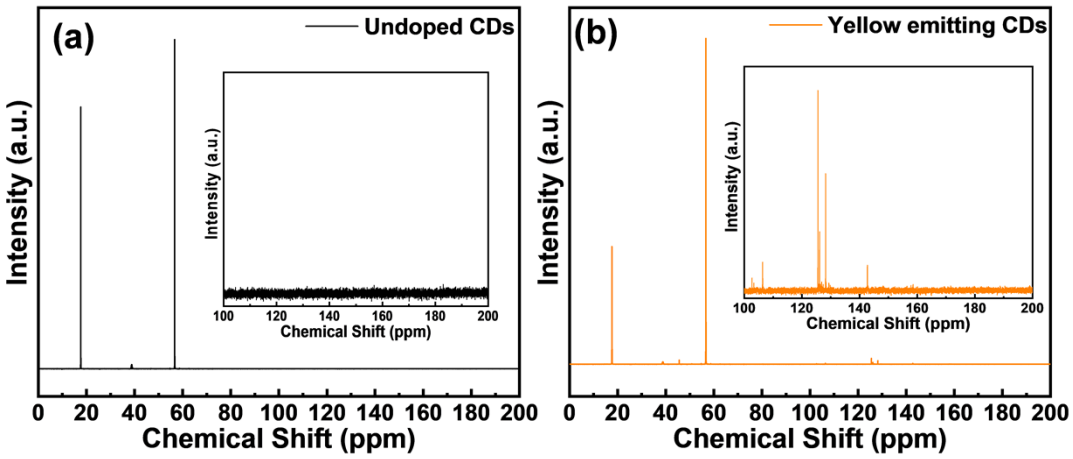

Figure S2. ^{13}C NMR spectra of undoped CDs (a) and yellow emitting CDs (b).

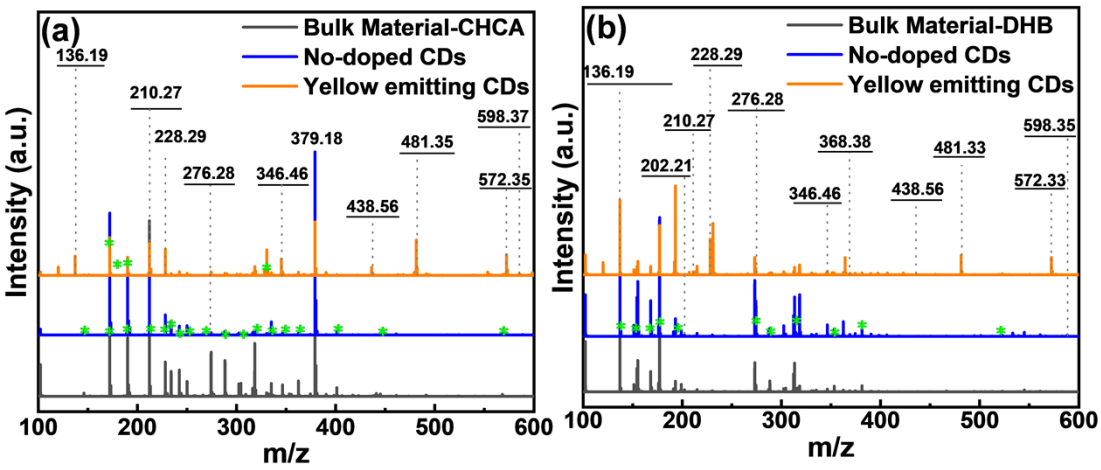

Figure S3. MS spectra of undoped CDs and yellow emitting CDs via the MALDI-TOF device. (a) The assisting matrix is the α-Cyano-4-hydroxycinnamic acid (CHCA). (b) The assisting matrix is the 2,5-Dihydroxybenzoic acid (DHB).

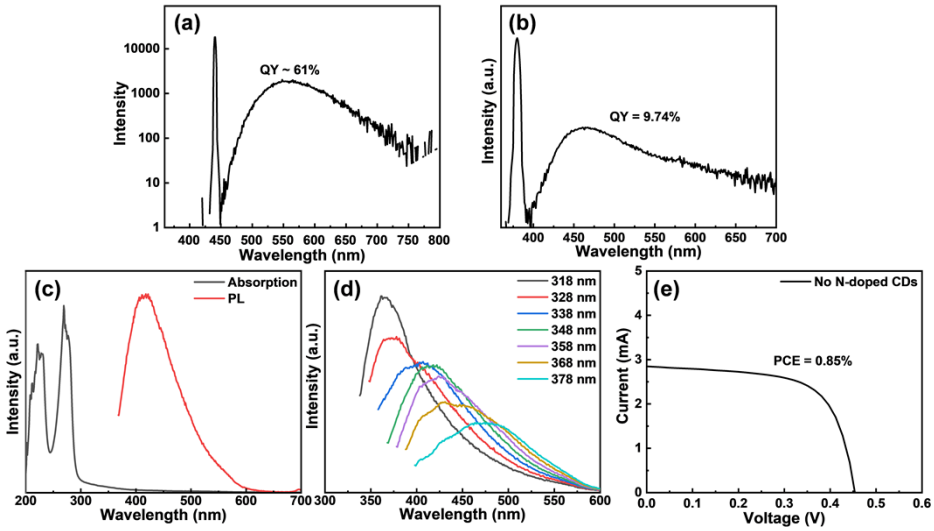

Figure S4. The measured QY of the yellow emitting CDs (a) and non N-doped CDs (b). (c) The absorption and emission spectra of the non N-doped CDs dispersed in ethanol solution. (d) The PL spectra of the non N-doped CDs under different excitation wavelength. (e) *J-V* response of the LSC based on non N-doped CDs.

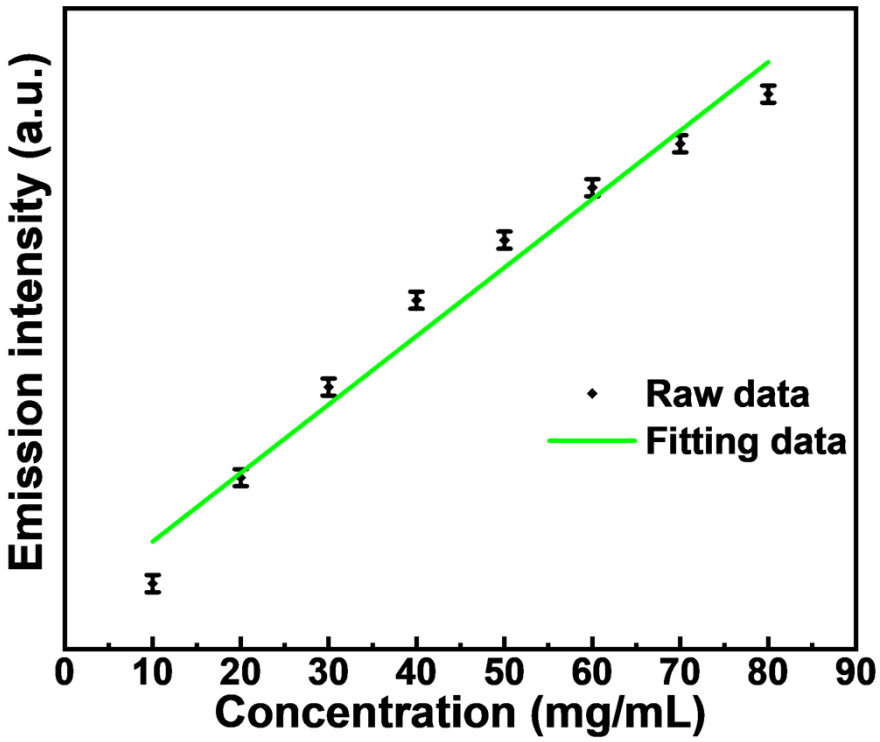

Figure S5. The relationship between emission intensity and concentrations.

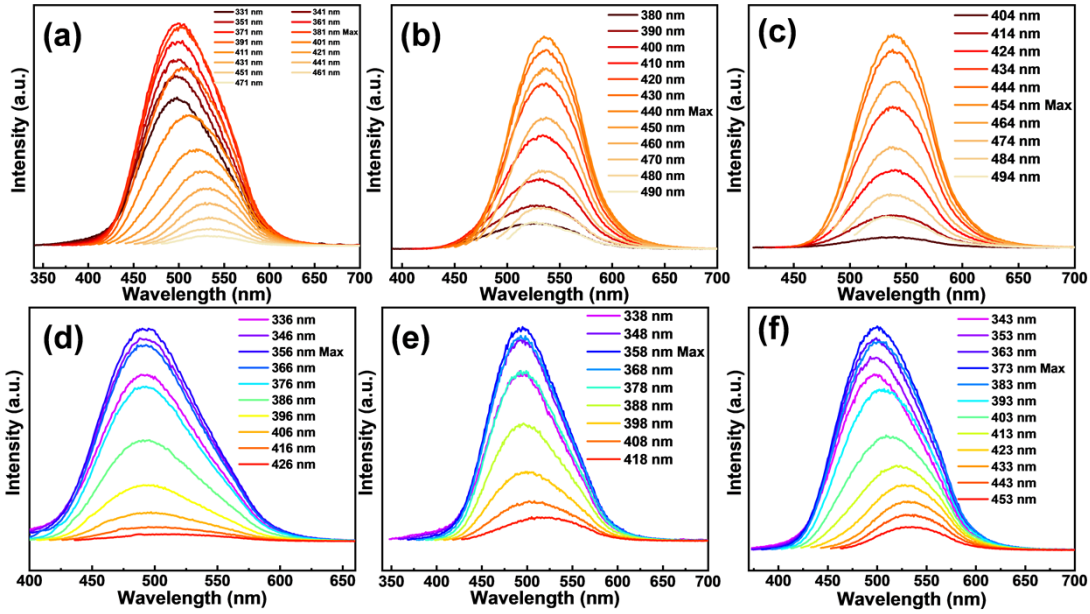

Figure S6. The PL spectra of the yellow emitting CDs under different excitation wavelengths in different concentrations. (a) 50 mg/mL, (b) 80 mg/mL, (c) 100 mg/mL, (d) 0.2 mg/mL, (e) 2 mg/mL, and (f) 5 mg/mL.

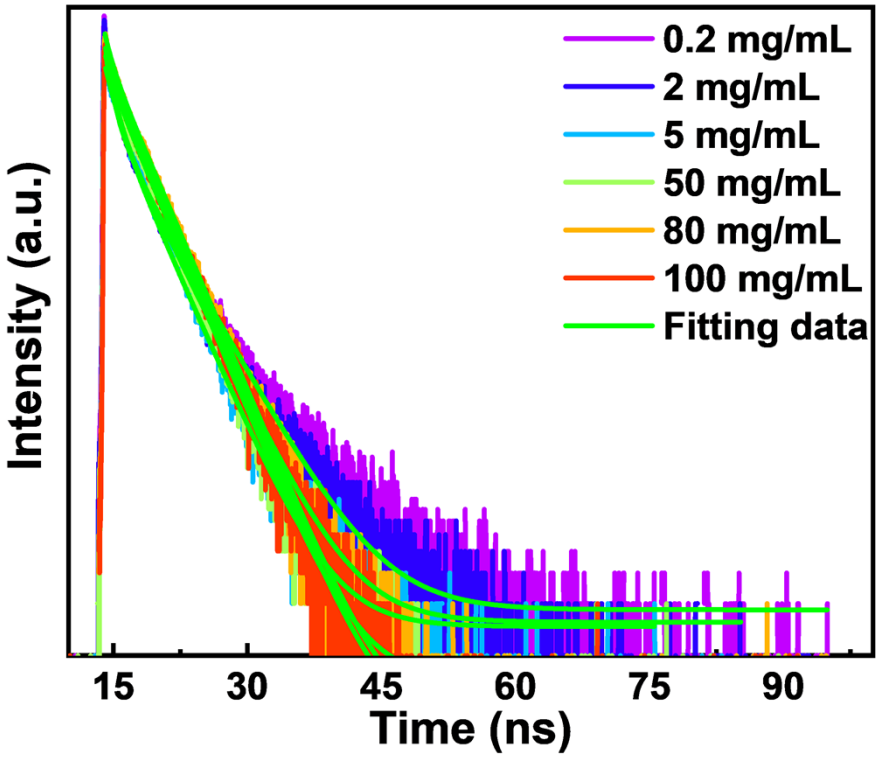

Figure S7. The emission decay of yellow emitting CDs with different concentrations under 460 nm excitation.

Table S1. The fluorescence lifetime for double exponential lifetimes of yellow emitting CDs with different concentrations under 460 nm excitation.

Concentration (mg/mL)	τ_1 (ns)	τ_2 (ns)	$\tau_{average}$ (ns)	R^2
0.2	1.12	4.76	3.82	0.998
2	0.70	4.06	3.39	0.997
5	1.23	3.70	3.24	0.996
50	0.84	3.53	3.38	0.998
80	0.83	3.59	3.40	0.999
100	0.91	3.58	3.41	0.999

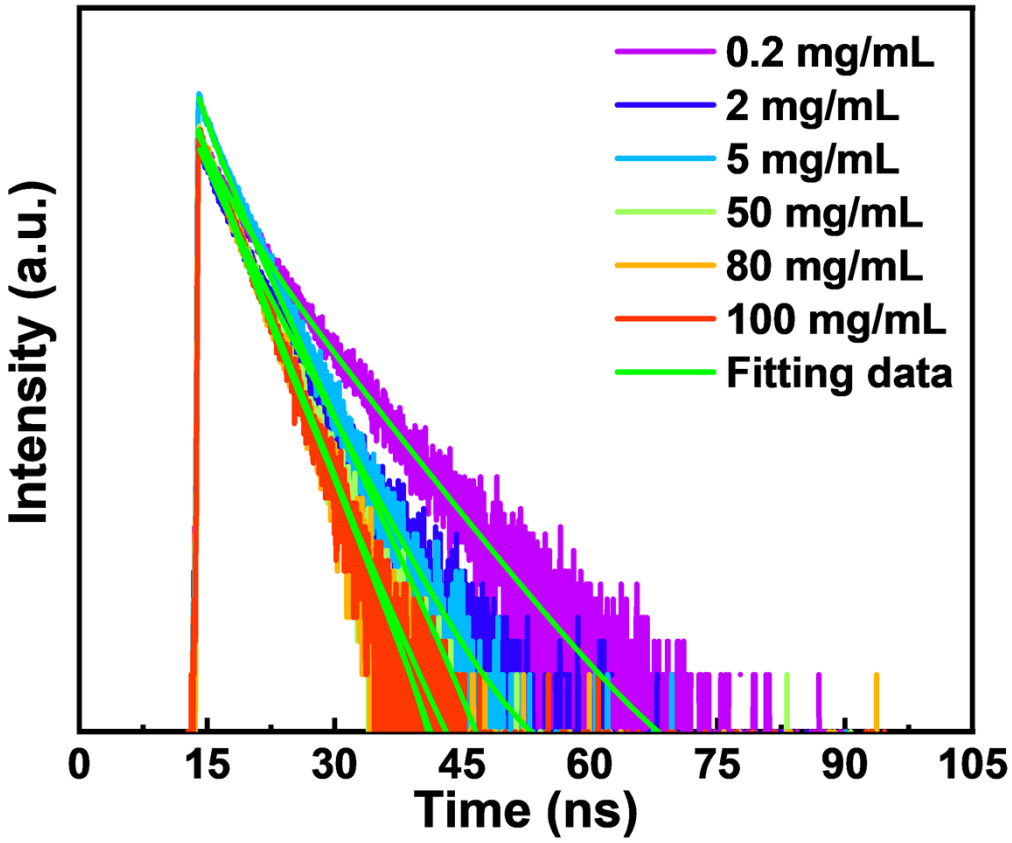

Figure S8. The emission decay of yellow emitting CDs with different concentrations under 360 nm excitation.

Table S2. The fluorescence lifetime for double exponential lifetimes of yellow emitting CDs in different concentrations under 460 nm excitation.

Concentration (mg/mL)	τ_1 (ns)	τ_2 (ns)	$\tau_{average}$ (ns)	R^2
0.2	3.02	7.75	6.70	0.995
2	2.01	5.18	4.93	0.997
5	2.18	4.60	4.14	0.996
50	2.46	4.19	3.74	0.995
80	1.52	3.97	3.84	0.998
100	3.43	4.10	3.80	0.998

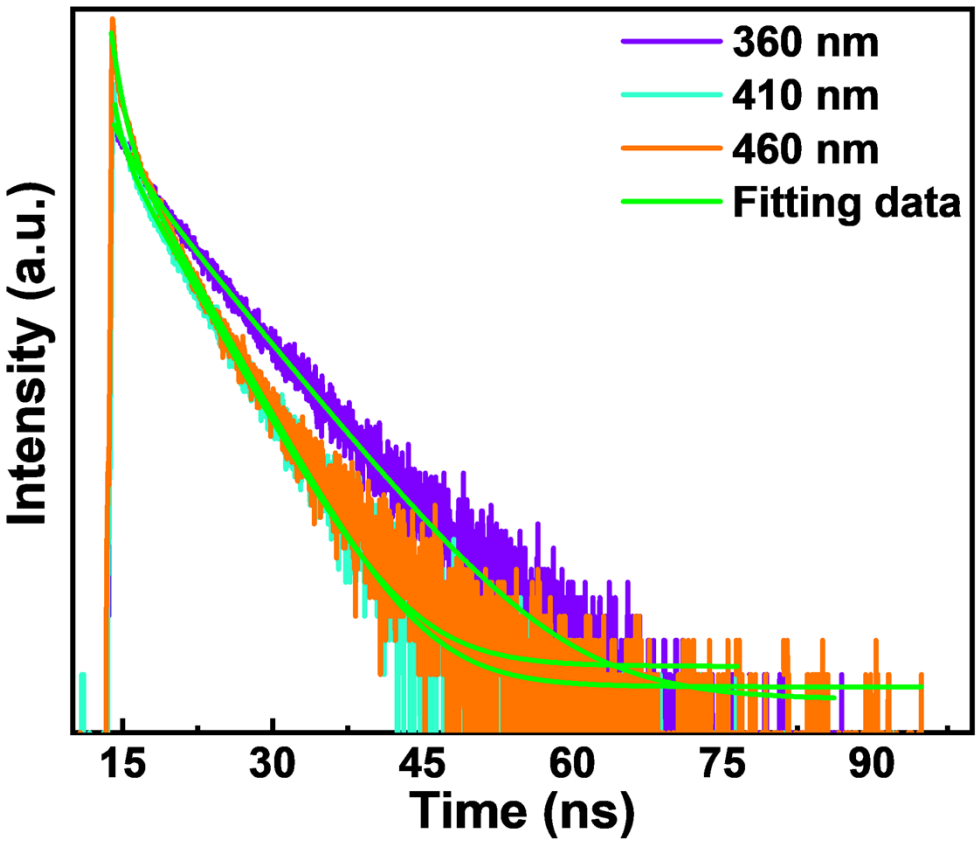

Figure S9. The emission decay of yellow emitting CDs with the concentrations of 0.2 mg/mL under different excitation.

Table S3. The fluorescence lifetime for double exponential lifetimes of yellow emitting CDs for the concentrations of 0.2 mg/mL at different excitation.

Excitation	τ_1 (ns)	τ_2 (ns)	$\tau_{average}$ (ns)	R^2
360 nm	1.94	6.95	6.44	0.998
410 nm	0.79	4.76	4.36	0.997
460 nm	0.89	4.51	3.59	0.996

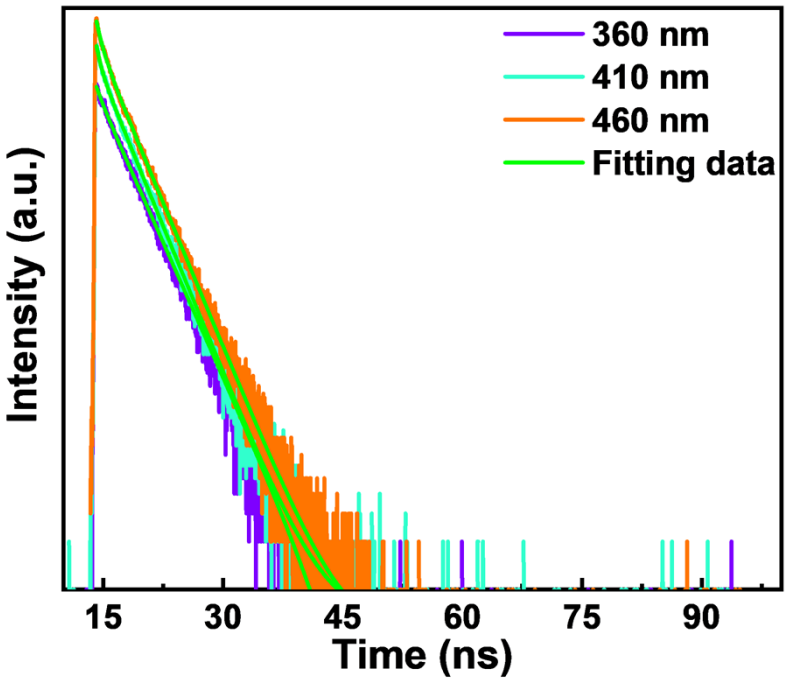

Figure S10. The emission decay of yellow emitting CDs with the concentrations of 80 mg/mL under different excitation.

Table S4. The fluorescence lifetime for double exponential lifetimes of yellow emitting CDs for the concentrations of 80 mg/mL at different excitation.

Excitation	τ_1 (ns)	τ_2 (ns)	$\tau_{average}$ (ns)	R^2
360 nm	0.83	3.86	3.81	0.998
410 nm	0.57	3.53	3.41	0.999
460 nm	0.77	3.59	3.39	0.999

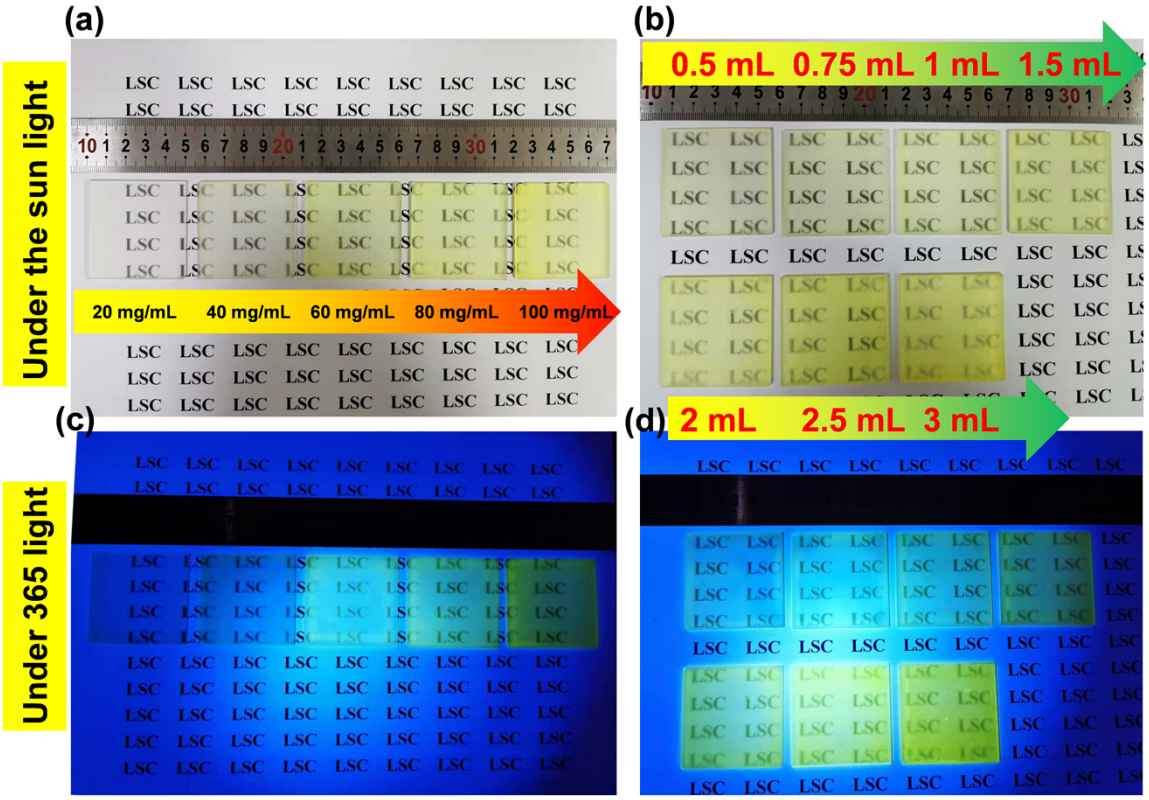

Figure S11. Photographs of the LSCs based on yellow emitting CDs.

Table S5. Photovoltaic parameters of yellow emitting CDs based LSC devices.

Concentration (mg/mL)	V_{oc} (V)	I_{sc} (A)	J_{sc} (mA/cm^2)	I_{max} (A)	V_{max} (V)	P_{max} (mW)	Fill Factor (%)	Efficiency (%)	G
Blank	0.54366	0.02729	36.87628	0.02508	0.44824	11.24008	75.76399	15.1893	6.25
20	0.50812	0.00591	7.99048	0.00532	0.41692	2.21788	73.81879	2.99713	6.25
40	0.51115	0.00673	9.09974	0.00607	0.42057	2.55165	74.13312	3.44817	6.25
60	0.51219	0.00717	9.68281	0.00647	0.42118	2.72534	74.26057	3.68289	6.25
80	0.5106	0.00727	9.82681	0.00657	0.41949	2.75526	74.20598	3.72332	6.25
100	0.50978	0.00728	9.83871	0.00657	0.41894	2.75296	74.17381	3.72021	6.25

Table S6. Photovoltaic parameters of yellow emitting CDs based LSCs devices.

Dosage	V_{oc} (V)	I_{sc} (A)	J_{sc} (mA/cm^2)	I_{max} (A)	V_{max} (V)	P_{max} (mW)	Fill Factor (%)	Efficiency (%)	G
Blank	0.54366	0.02729	36.87628	0.02508	0.44824	11.24008	75.76399	15.1893	6.25
0.5 mL	0.50063	0.00645	8.72342	0.00581	0.41008	2.381	73.67521	3.21756	6.25
0.75 mL	0.50107	0.00653	8.82302	0.00587	0.40957	2.40549	73.52822	3.25067	6.25
1.0 mL	0.5031	0.00687	9.28869	0.0062	0.41074	2.54673	73.64508	3.44153	6.25
1.5 mL	0.50504	0.00737	9.95367	0.00665	0.414	2.75155	73.96676	3.71831	6.25
2.0 mL	0.5077	0.008	10.81157	0.00722	0.41747	3.01471	74.21908	4.07393	6.25
2.5 mL	0.50769	0.00814	11.00571	0.00734	0.41711	3.06277	74.07433	4.13888	6.25
3.0 mL	0.50265	0.00691	9.33387	0.0062	0.41151	2.55272	73.52674	3.44962	6.25

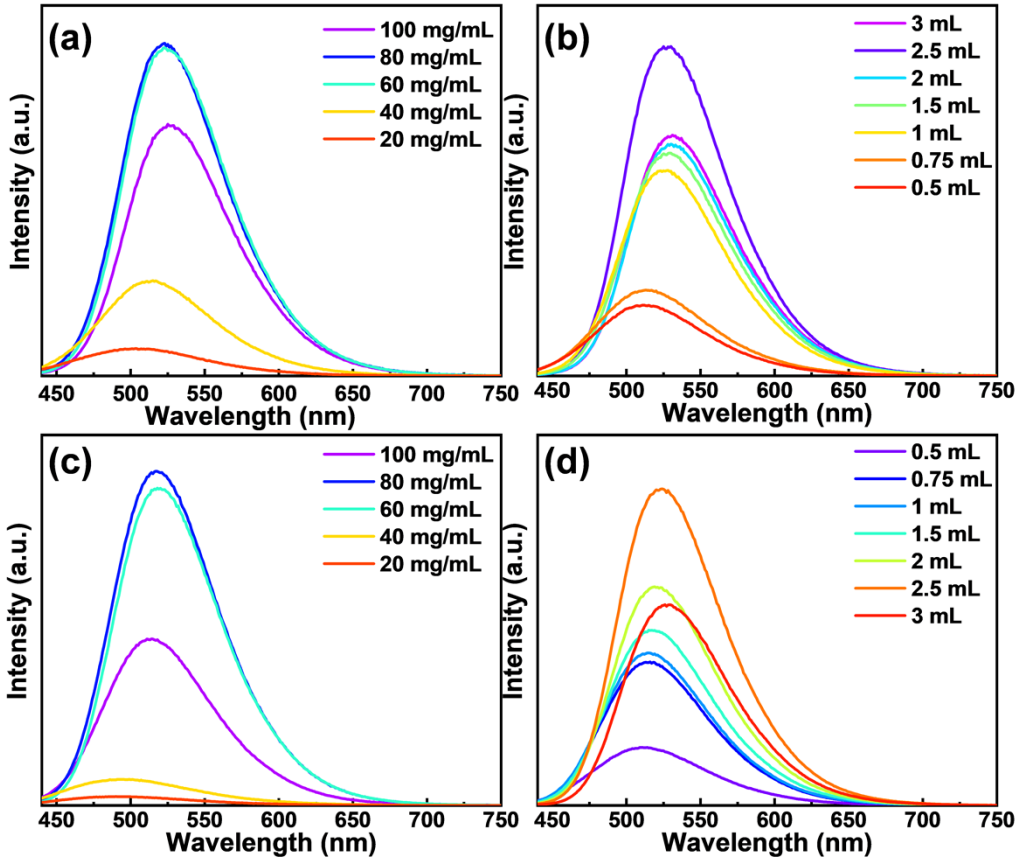

Figure S12. (a) The PL spectra of the LSCs with the concentration of yellow emitting CDs of 80 mg/mL. (b) The PL spectra of the LSCs with the dosage of 2.5 mL. (c) The PL spectra of the LSCs with the concentration of yellow emitting CDs of 80 mg/mL after five weeks. (d) The PL spectra of the LSCs with the dosage of 2.5 mL after five weeks.

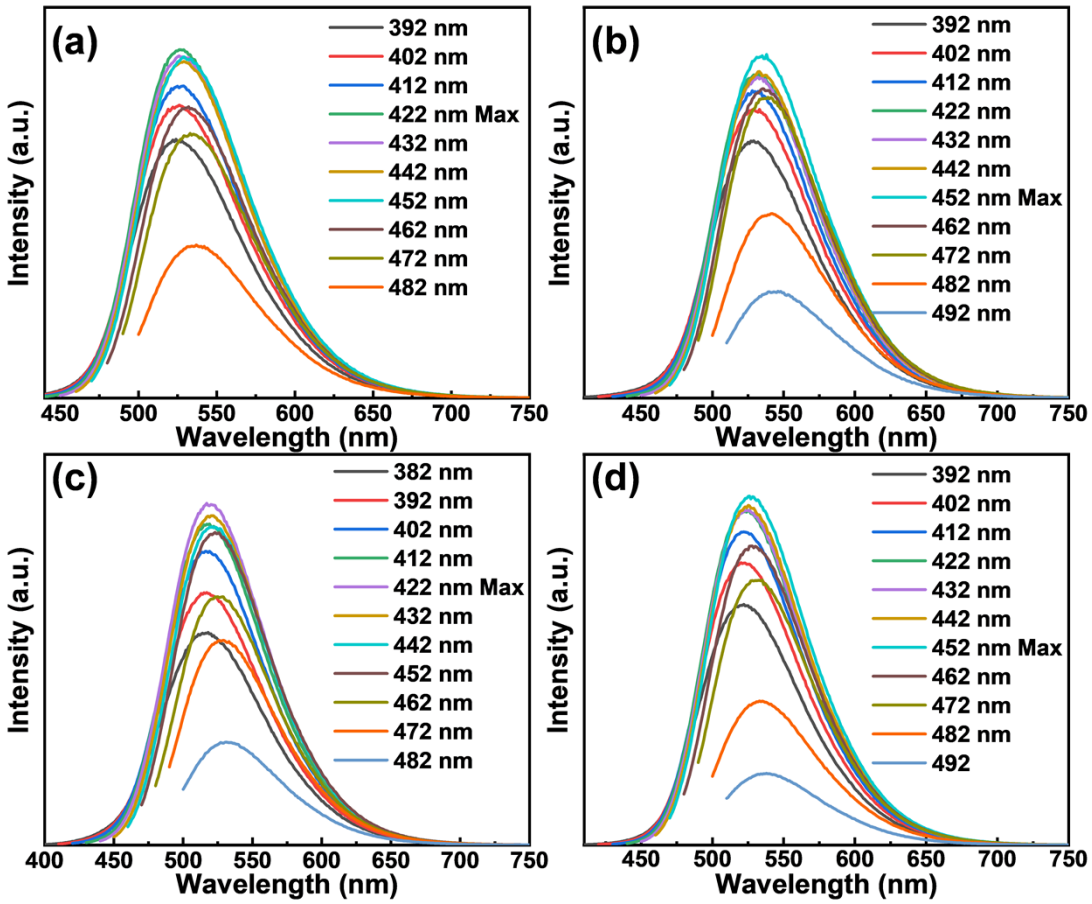

Figure S13. (a) The PL spectra of the LSCs with the concentration of yellow emitting CDs of 80 mg/mL under different excitation wavelengths. (b) The PL spectra of the LSCs with the dosage of 2.5 mL under different excitation wavelengths. (c) The PL spectra of the LSCs with the concentration of yellow emitting CDs of 80 mg/mL after five weeks under different excitation wavelengths. (d) The PL spectra of the LSCs with the dosage of 2.5 mL after five weeks under different excitation wavelengths.

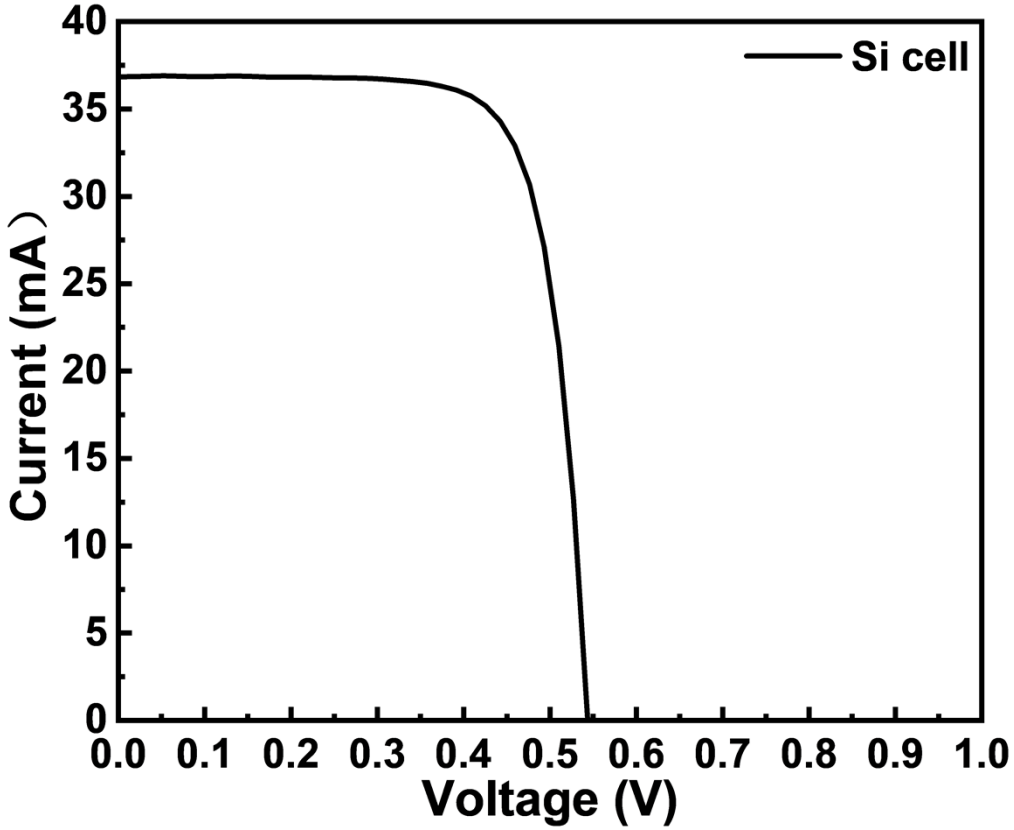

Figure S14. The photocurrent density and photovoltage (*J-V*) response of the Si solar cell.

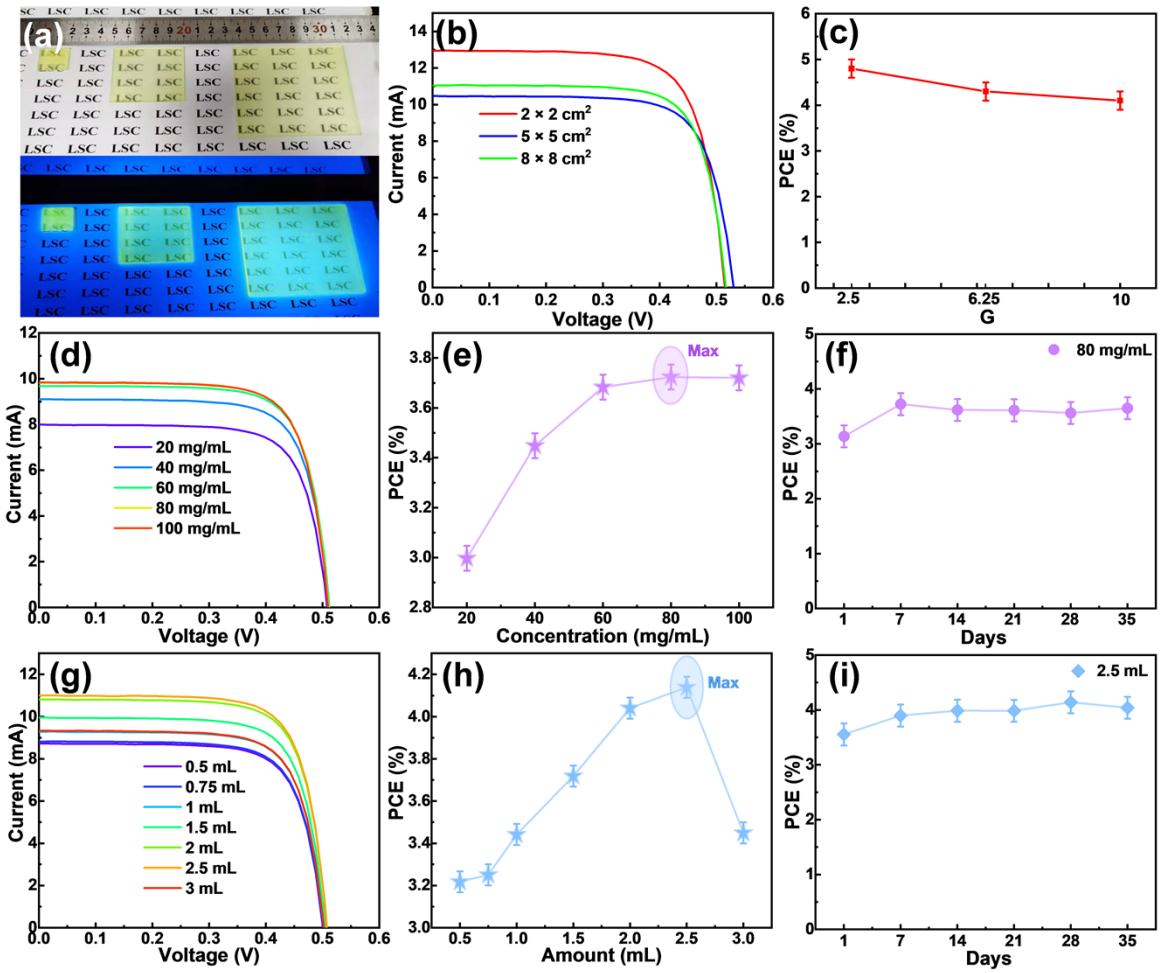

Figure S15. (a) Optical pictures of LSCs in different sizes. (b) *J-V* response of the LSC under the different sizes. (c) The relationship of PCE under the different G factor. (d) *J-V* response of the LSC under the different concentrations. (e) The relationship of PCE under the different concentrations. (f) Stability of PCE at different concentrations. (g) *J-V* response of the LSC under the different dosage. (h) The relationship of PCE under the different dosage. (i) Stability of PCE at different dosage.

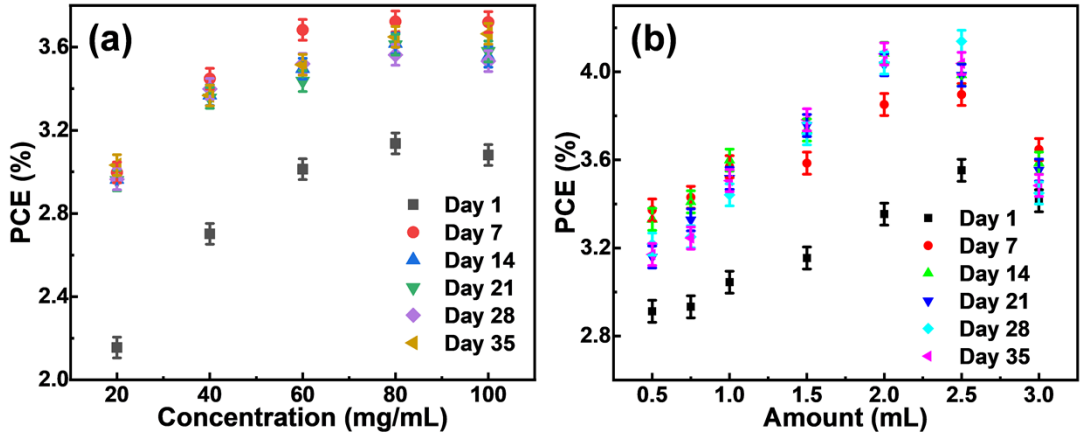

Figure S16. Stability of PCE of LSCs with different concentrations and different dosage.

References:

1. V. I. Klimov, T. A. Baker, J. Lim, K. A. Velizhanin and H. McDaniel, *ACS Photonics*, 2016, **3**, 1138-1148.

2. F. Mateen, M. Ali, H. Oh and S.-K. Hong, *Solar Energy*, 2019, **178**, 48-55.

3. Y. Han, X. Zhao, A. Vomiero, X. Gong and H. Zhao, *Journal of Materials Chemistry C*, 2021, **9**, 12255-12262.

4. H. Zhao, G. Liu, S. You, F. V. A. Camargo, M. Zavelani-Rossi, X. Wang, C. Sun, B. Liu, Y. Zhang, G. Han, A. Vomiero and X. Gong, *Energy & Environmental Science*, 2021, **14**, 396-406.